Summer Student Program 2003 Report

Jan Becker

September 4, 2003

Contents

1 Introduction **3**

2 Properties of Silicon Detectors **4**

3 Experimental Techniques **7**
3.1 CV/IV-Measurements 7
3.1.1 CV-Measurement 7
3.1.2 IV-Measurement 7
3.2 TCT-Measurements 8

4 Experimental Results **10**

5 Conclusions **21**

List of Tables

1 Names of the devices and electron fluences considered 10
2 Thickness and $N_{eff,0}$ of the devices 11
3 Values of κ 13
4 Annealing time at which type inversion occurs 13
5 Values of parameters for ΔN_{eff} if devices are inverted from beginning 17
6 Values of parameters for ΔN_{eff} if devices invert during annealing 17
7 Values of parameters for the fit of ΔN_{eff} as a function of the fluence 20

List of Figures

1 Relation between Depletion Voltage and Fluence 5
2 Depletion Voltage after years 5
3 CV characteristic fit to calculate the depletion voltage 7
4 Schematic view of TCT operation 8
5 Electron injection from the front contact 9
6 Hole injection from the rear contact 9
7 Trend of the electric field in the device 10
8 Dependence of the depletion voltage on the annealing time . . 12
9 Dependence of α_{el} on the annealing time 12
10 Find out type inversion with IV-measurement 14
11 TCT: front injection for a non-inverted device 15
12 TCT: back injection for non-inverted device 15
13 TCT: front injection for an inverted device 16
14 TCT: back injection for an inverted device 16
15 ΔN_{eff} of CA0510, if inverted from the beginning 18
16 ΔN_{eff} of CA0510, if inverted after 60 minutes of annealing . . 18
17 ΔN_{eff} of CD1710, if inverted from the beginning 19
18 ΔN_{eff} of CD1710, if inverted after 90 minutes of annealing . . 19
19 N_{eff} relation to the fluence 20

1 Introduction

The research topic presented in this work, performed in the context of the DESY Summer Student Program, concerns the radiation tolerance of silicon detectors. In high-energy physics experiments silicon detectors are widely used as microstrip detectors, or pixel detectors in tracking chambers. They can achieve a position resolution down to a few μm. That is the best possible resolution at the moment. Because of this high precision these silicon detectors are usually the innermost layers of the tracking detectors. However that means that they are exposed to a very high radiation flux, i.e. at the LHC experiment a radiation of up to several 10^{14} hadrons/cm^2 per year is expected, and it is foreseen that the detectors should operate for 10 years. Radiation damage change the properties of silicon detectors. For example the depletion voltage changes, the leakage current increases and the charge collection efficiency decreases. The substrate can undergo the so-called typer inversion (inversion of the sign of the spatial charge. These changes depend on the silicon material, the kind of particles irradiating the material, on the energy of these particles and on the total fluence the detector is exposed to. As the production of silicon detectors is very expensive, solid state physicists develop and analyze different silicon materials to make them more resistant against radiation. For example an enrichment of the silicon bulk material with oxygen is a good solution to increase the radiation hardness (so-called Diffusion Oxygenated Float Zone (DOFZ) technology).
If irradiated silicon detectors are left at room temperature the thermal movement of atoms and defects has the effect that the silicon will recover its properties. Although silicon detectors have very low working temperatures, i.e. at ALTAS at LHC it will be -6 ℃, this annealing process has to be considered. The experiments will only run a few months a year. During the other months the whole detector will be at room temperature and it is opened for updates and repairs. To make a prediction about the properties of the silicon detectors after several years the annealing time has to be considered. Because it is very tough to wait for several months this annealing time has to be simulated. This can be done if the silicon devices are put into an oven. For example one minute at 60 ℃ in the oven simulates 8 hours at room temperature and one minute at 80 ℃ simulates 3.5 days at room temperature. In this work we investigated silicon devices irradiated with low energy (15 MeV) electrons. The used experimental techniques were capacitance-voltage (CV) and current-voltage (IV) measurement during annealing and Transient Current Technique (TCT) measurements to ascertain the sign of the electric field inside the detector.

2 Properties of Silicon Detectors

Radiation can induce in silicon detectors point defects or defect clusters. Point defects (threshold energy about 25 eV) can be created by low-energy recoils, e.g. neutrons with an energy above 175 eV or electrons with an energy above 260 keV. If the recoil energy is above 5 keV a dense agglomeration of defects will be created. For the production of such defect clusters, the radiation particles need an energy above 35 keV for neutrons and 8 MeV for electrons.
These defects can affect the detector performances and, depending on their concentration, the energy levels and the respective cross-sections for electron and hole capture. In particular the formation of complex defects is responsible for the removal of dopants and therefore also responsible for the change of the effective doping concentration, which also causes the depletion voltage to change.

At the depletion voltage the silicon is fully depleted, equivalent to the absence of free-carriers in the bulk material. The depletion voltage and the effective doping concentration N_{eff} are related by following equation:

$$V_{dep} = \frac{q_0}{2\epsilon\epsilon_0} \cdot |N_{eff}| \cdot d^2 \tag{1}$$

with:
q_0: elementary charge
$\epsilon\epsilon_0$: electric permittivity
d: thickness of the dectector
$|N_{eff}| = |N_d - N_a|$ where:
N_d: positively charged donor concentration
N_a: negatively charged donor concentration
This equation is valid for the original n-type silicon detector as well as for the irradiated detector also when the effective doping concentration changes its sign (inversion).

As shown in Fig. 1 the depletion voltage increases strongly after type inversion. This property is a major issue in the radiation hardening of silicon detectors.

Radiation hardness can be improved by defect engineering, which means an addition of impurities to reduce the electrically active defects. Many tests have shown that an oxygen enrichment by post-oxidation diffusion into the silicon is the best method.

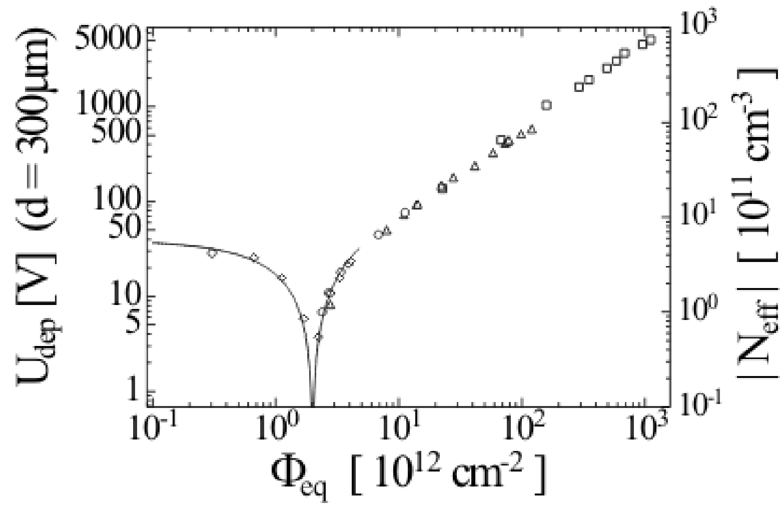

Figure 1: Change of the effective doping concentration in standard silicon, as measured immediately after neutron irradiation

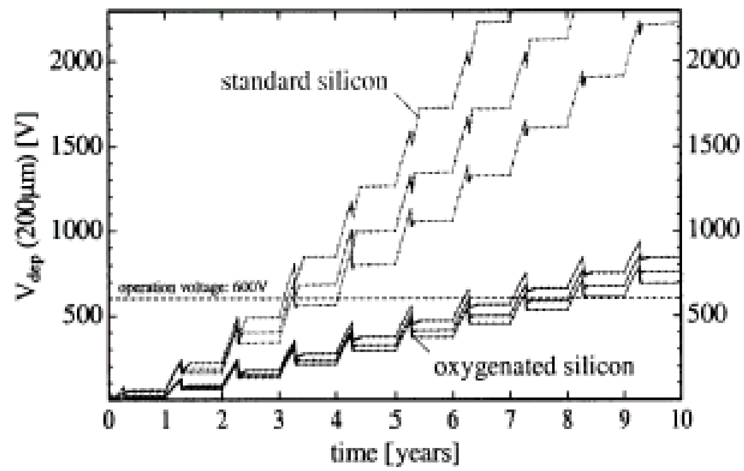

Figure 2: Damage projections for the silicon detector at ATLAS

Fig. 2 shows an example of prediction for the change in the depletion voltage of silicon detectors after 10 years of operating at LHC. It can be clearly seen that only DOFZ detectors can be used for the required 10 years, if the operational voltage will be 600 V.

3 Experimental Techniques

3.1 CV/IV-Measurements

All measurements has been made in the dark in a closed box, at atmospheric pressure and at room temperature. Reverse bias characteristics were typically recorded by increasing the voltage from small to large values within a few minutes, so that the sample and the instruments can settle at a given point for a sufficiently long time.

3.1.1 CV-Measurement

At full depletion voltage V_{dep} the junction capacitance C becomes constant. A slight reduction even beyond full depletion is often observed, mainly arising from the lateral expansion of the electric field zone. The CV characteristics is fitted with two straight lines, one in the range of V above V_{dep}, and the other one below V_{dep}. V_{dep} is then determined by the intersection of the two fits. This is the usual way to get a reproducible value for V_{dep}. An example of this is shown in Fig. 3.

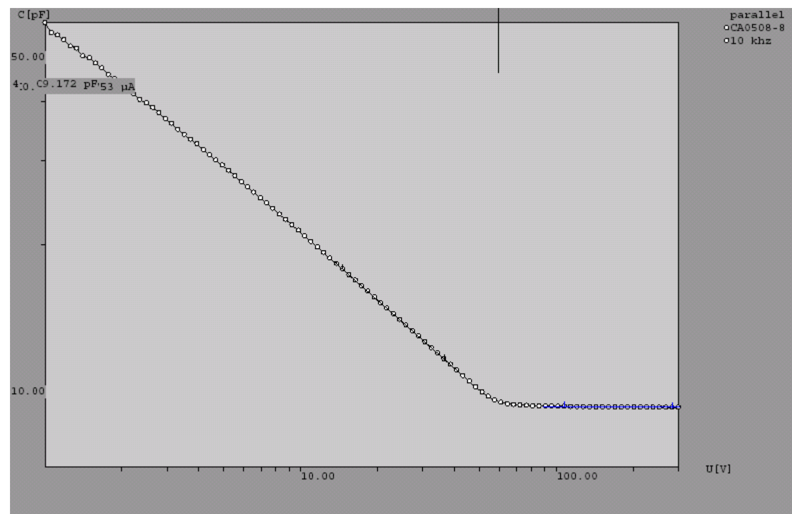

Figure 3: CV characteristic fit to calculate the depletion voltage

3.1.2 IV-Measurement

An estimation of the device leakage current is usually performed by interpolating the IV characteristics at the previously obtained depletion voltage

V_{dep} $(I_D = I(V_{dep}))$.

If the volume current is dominating, the leakage current gets (more or less) flat above full depletion. As the experimental data were taken at room temperature, which is not constant, it is important to consider that the IV data have been normalized to 20 ℃ to make a comparison at a later point possible.

3.2 TCT-Measurements

In TCT-measurements, a short laser pulse generates free carriers. The used laser has a wavelength of $\lambda = 670$ nm which results in a penetration depth of $\alpha_{abs}(293\ \mathrm{K}) = 3.3\ \mu$m, so that electron-hole pairs are created very close to the front or rear contact of the detector. Therefore only electrons or holes will travel across the whole detector. The complementary charge carriers will be collected by the adjacent electrode. This is the reason why laser injection from the backside is called hole-injection and injection from the front side is called electron-injection. A schematic view of the laser injection is shown in Fig. 4.

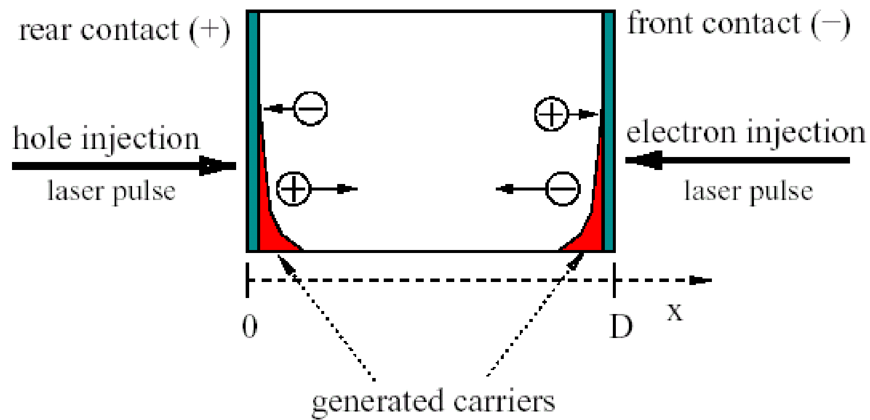

Figure 4: Schematic view of TCT operation

During the measurement the current pulse induced at the electrode by the injected carriers is recorded as a function of the bias voltage.
The main difference between electron and hole injection is in the carriers drift

velocity. For electrons, it is large in the beginning and decreases towards the end of the drift, which shows that there is a strong electric field at the front contact and a weaker one at the back contact. Because holes are created at the other side of the device their drift velocities will increase during their passage. A schematic view of electron injection with a laser diode from the front contact is shown in Fig. 5, and of hole injection from the rear contact in Fig. 6.

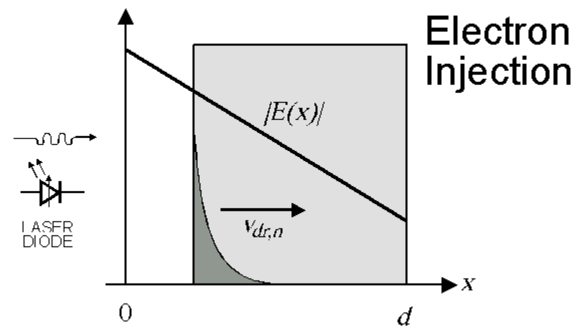

Figure 5: Electron injection from the front contact

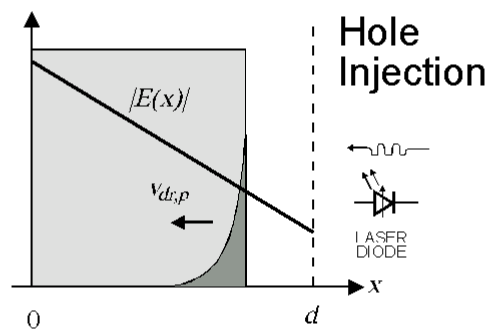

Figure 6: Hole injection from the rear contact

If the detector is inverted the drift velocity of electrons will decrease with the drift time, while the drift velocity of holes will increase, because the electric field increases in the other direction. This is shown in Fig. 7.

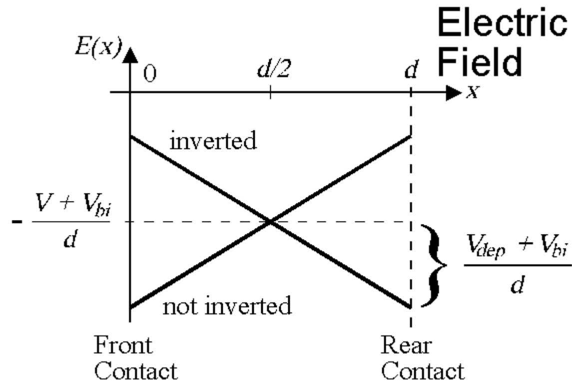

Figure 7: Trend of the electric field in the device

4 Experimental Results

The work we have done was to analyze how the depletion voltage and the leakage current of irradiated silicon devices change as a function of the annealing time. We also compared the differences in the properties when the devices were irradiated with different fluences. In addition we compared the behavior of oxygen enriched and non-enriched silicon devices. For this research I had four different devices. All of them were Float Zone silicon but two of them were enriched for 72 hours at 1150 ℃ with oxygen (DOFZ silicon). One of each type was irradiated by $4.65 \cdot 10^{13}$ $1/\text{cm}^2$ and the other two by $4.65 \cdot 10^{14}$ $1/\text{cm}^2$ electrons with an energy of 15 MeV.

Name of Device	Oxygenation	fluence [electrons/cm^2]
CA0508	non-enriched	$4,65 \cdot 10^{13}$
CD1708	enriched	$4,65 \cdot 10^{13}$
CA0510	non-enriched	$4,65 \cdot 10^{14}$
CD1710	enriched	$4,65 \cdot 10^{14}$

Table 1: Names of the devices and electron fluences considered

Before irradiating the samples, a CV-Measurement has been done on all the samples. From this measurement the depletion voltage and the final constant capacitance C_{end} of the devices has been determined. With the following equations it is possible to calculate the thickness d and the initial effective doping concentration $N_{eff,0}$:

$$C_{end} = \epsilon \cdot \epsilon_0 \cdot \frac{A}{d}$$

and

$$V_{dep} = \frac{q_0}{2\epsilon\epsilon_0} \cdot |N_{eff}| \cdot d^2$$

with: $q_0 = 1,602 \cdot 10^{-19}$C, $\epsilon = 11,8$, $\epsilon_0 = 8,85419 \cdot 10^{-14} \frac{\mathrm{F}}{\mathrm{cm}}$ and $A = 0,25\ cm^2$
The results are shown in Table 2.

Name of Device	thickness d	$N_{eff,0}[\mathrm{cm}^{-3}]$
CA0508	$283,6 \cdot 10^{-4}$ cm	$1,141 \cdot 10^{12}$
CD1708	$273,7 \cdot 10^{-4}$ cm	$8,058 \cdot 10^{11}$
CA0510	$283,8 \cdot 10^{-4}$ cm	$1,134 \cdot 10^{12}$
CD1710	$280,0 \cdot 10^{-4}$ cm	$7,861 \cdot 10^{12}$

Table 2: Thickness and $N_{eff,0}$ of the devices

After irradiation the samples have been annealed in an oven at 80 ℃, and the depletion voltage V_{Dep} and the leakage current I_D have been measured as a function of the annealing time. The distribution of the depletion voltage for all four devices is shown in Fig. 8.

For the lower irradiated samples a slight decrease in the depletion voltage as a function of the annealing time was detected. The higher irradiated samples first have a minimum in the depletion voltage and then increase at higher annealing times. For the DOFZ silcon the minimum is later than for the standard FZ silicon.
With the IV-measurement it is possible to determine the current at full depletion voltage which we take as an estimation of the leakage current. The following equation allows the calculation of the leakage current density increase rate α_{el} in dependence of the annealing time:

$$\alpha_{el}(t) \cdot \Phi_{el} = \frac{I_D(t)}{V} = \frac{I_D(t)}{A \cdot d} \tag{2}$$

Fig. 9 shows the results of the four devices. As expected for all four devices α_{el} becomes a linear trend.

Φ_{eq} is the equivalent fluence of 1 MeV neutron irradiation:

$$\Phi_{eq} = \kappa \cdot \Phi_{el}$$

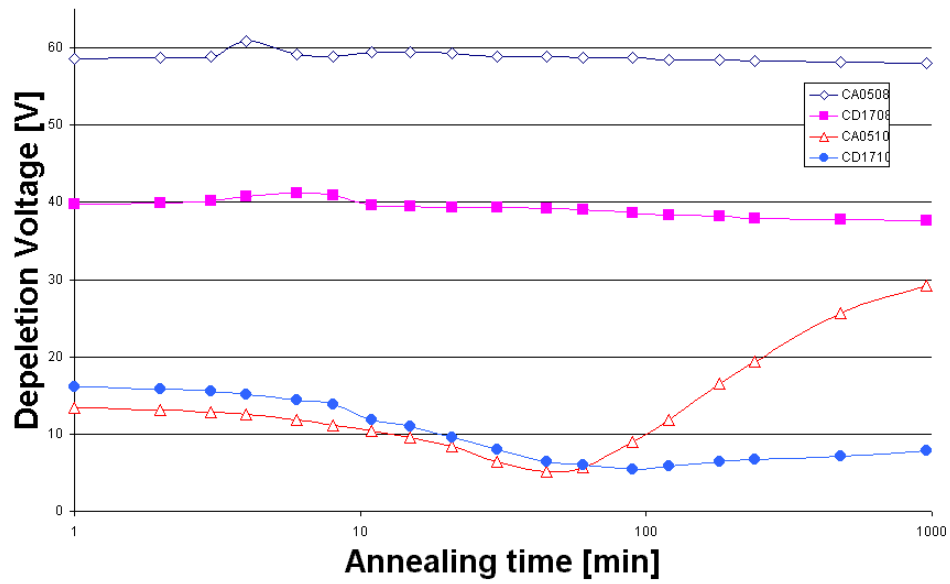

Figure 8: Dependence of the depletion voltage on the annealing time

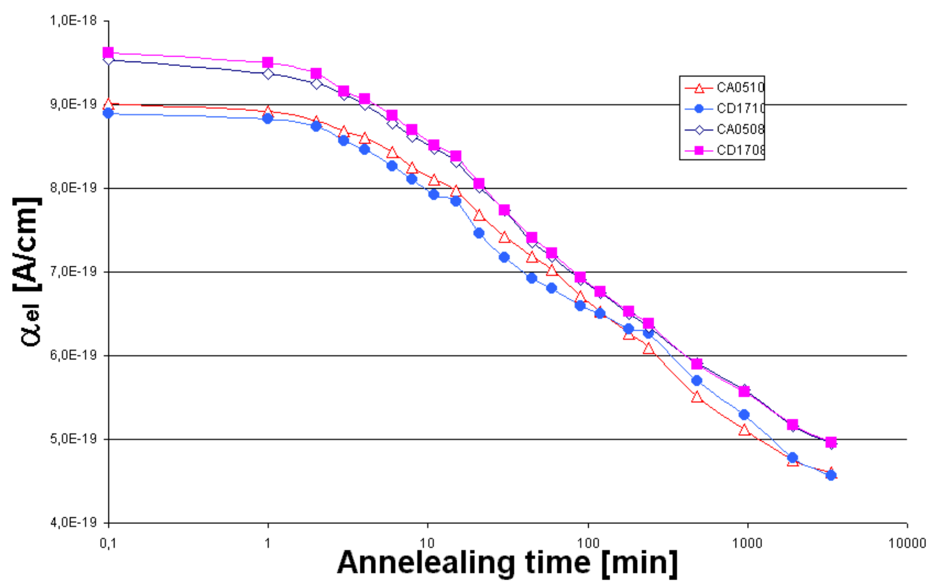

Figure 9: Dependence of α_{el} on the annealing time

Name of Device	κ
CA0508	0,02154
CD1708	0,02173
CA0510	0,02064
CD1710	0,02026

Table 3: Values of κ

where Φ_{el} is the fluence at which the devices were irradiated. The hardness factor κ can be calculated from α_{el}. It is standard to calculate α_{el} by equation 2 on page 11 after an annealing time of 8 at 80 ℃ minutes. The different values for κ are shown in Tab. 3.

IV-measurement is also useful to find out after what time the silicon detector is type inverted. Fig. 10 shows the IV-measurement for the CA0510 device after three different annealing times. After 8 minutes the IV curve has a round trend. But after 60 minutes of annealing a very small bump in the curve can be seen. This bump is a clear indicator that the device is type inverted, because the depletion now arises from the back side of the device and the guard-ring on the front side now influences the current characteristics. After 960 minutes of annealing the bump is very clearly seen, so somewhere in between the device inverted.

With TCT measurements it is easier to see if a device is inverted or not. It is only necessary to look at the slope of the experimental curves. Electron and hole injections have opposite characteristics. Fig. 11 and 12 show a non-inverted device with electron injection and hole injection. TCT measurements of type inverted devices are shown in Fig. 13 and 14.

With this two methods the annealing time for type inversion were determined, as shown in Tab. 4

Name of Device	annealing time
CA0508	not inverted
CD1708	not inverted
CA0510	$\sim$ 60 minutes
CD1710	$\sim$ 90 minutes

Table 4: Annealing time at which type inversion occurs

Another useful value for comparison is ΔN_{eff}:

$$\Delta N_{eff} = N_{eff,0} - N_{eff}\left(\Phi_{el}, t\right)$$

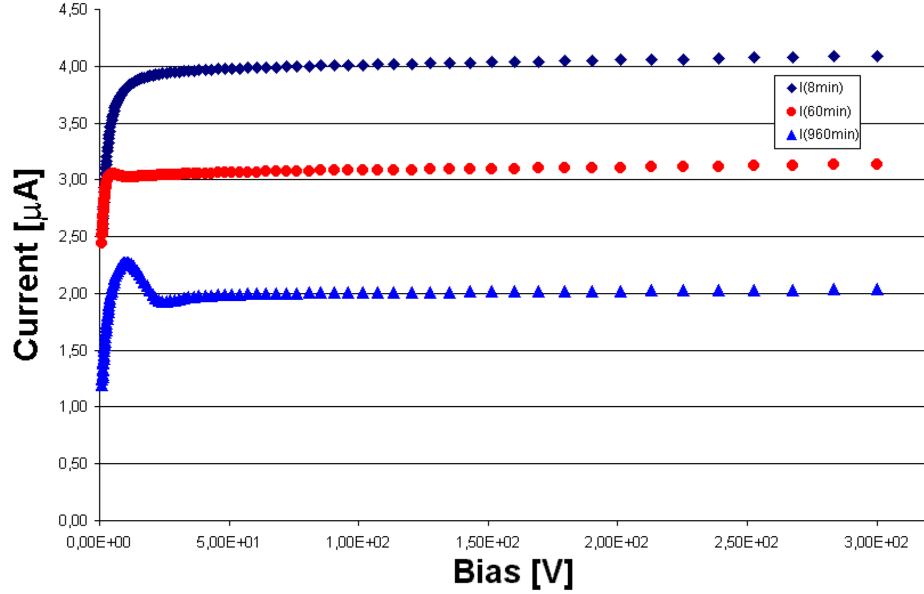

Figure 10: Find out type inversion with IV-measurement

N_{eff} can be calculated by equation (1) on page 4, if the depletion voltage was measured.
There is also a theoretical way to calculate ΔN_{eff}, according to the so-called "'Hamburg Model"':

$$\Delta N_{eff}(\Phi,t) = N_A(\Phi,t) + N_C(\Phi) + N_Y(\Phi,t) \tag{3}$$

with:

$$N_A = N_a \cdot \exp\frac{-t}{\tau_1} \qquad \text{beneficial annealing}$$

$$N_C = N_{C,0}\left(1 - \exp\left(-c \cdot \Phi_{eq}\right)\right) + g_c \cdot \Phi_{eq}$$

(1.term: donor removal 2.term: acceptor creation)

$$N_Y = N_{Y,\infty}\left(1 - \exp\left(\frac{-t}{\tau_2}\right)\right) \qquad \text{(1st order process of reverse annealing)}$$

$$N_Y = N_{Y,\infty}\left(1 - \frac{1}{1+\frac{t}{\tau_2}}\right) \qquad \text{(2nd order process of reverse annealing)}$$

Both equations have 5 parameters. They were determined by fitting the curve through the experimental values calculated from the depletion voltage. The 2. order process is used for the values measured directly after annealing,

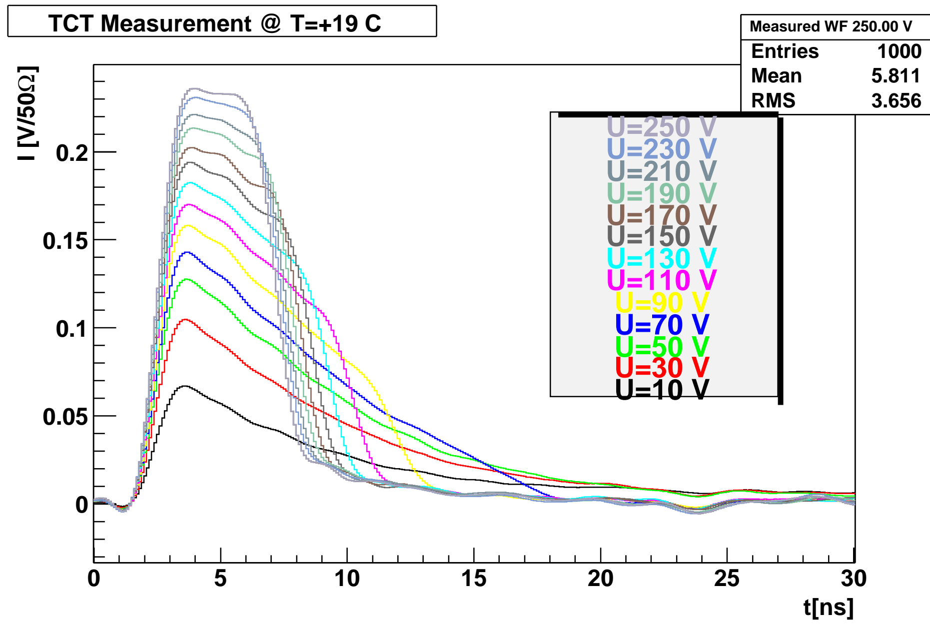

Figure 11: TCT: front injection for a non-inverted device: CD1708 at 8 minutes of annealing

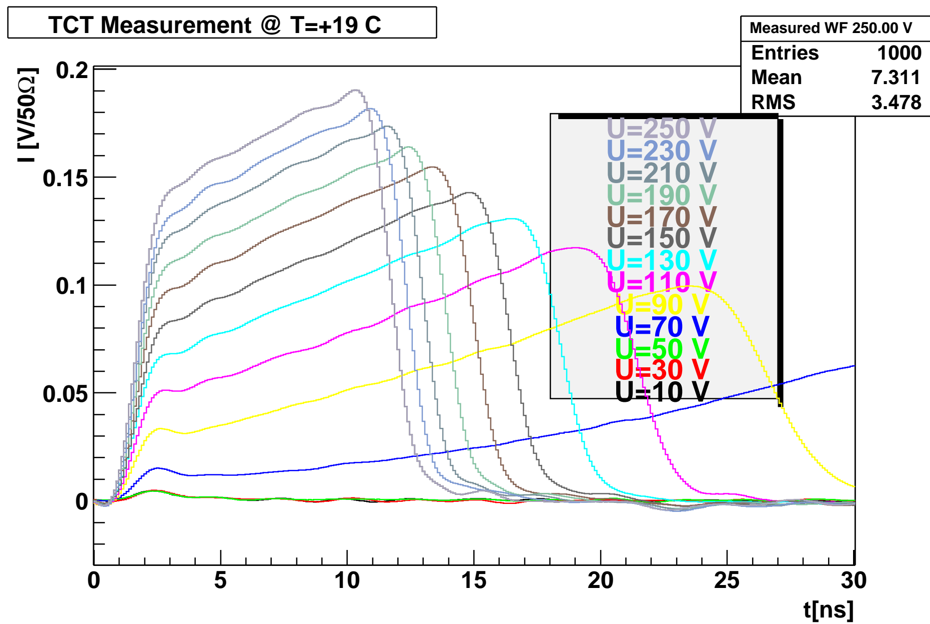

Figure 12: TCT: back injection for non-inverted device: CD1708 at 8 minutes of annealing

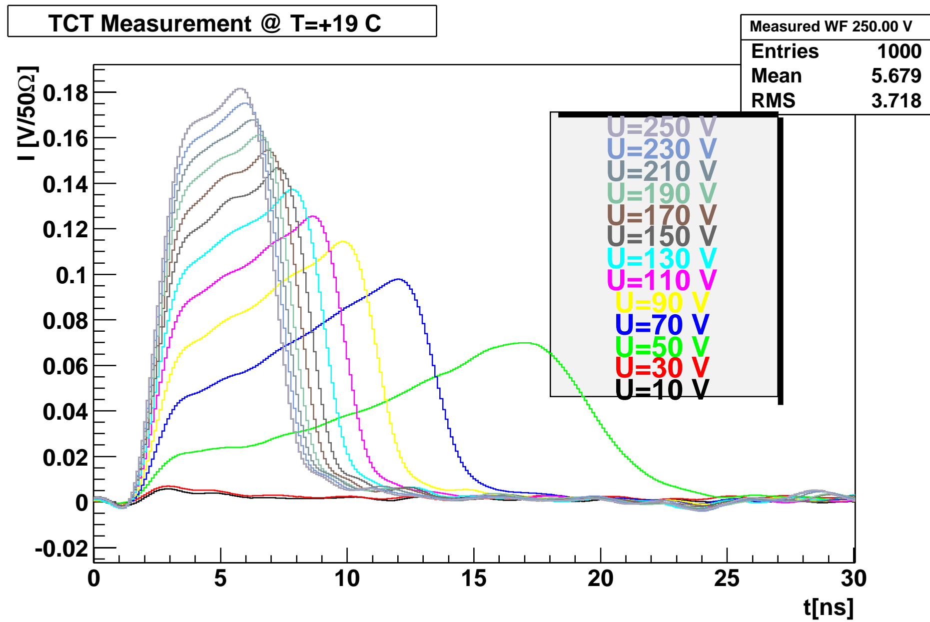

Figure 13: TCT: front injection for an inverted device: CA0510 at 960 minutes of annealing

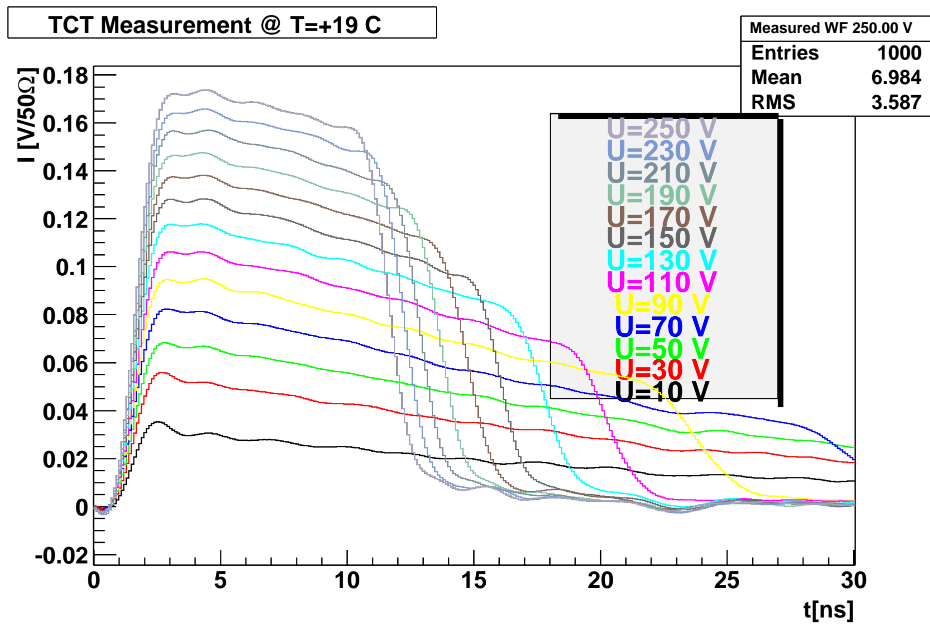

Figure 14: TCT: back injection for an inverted device: CA0510 at 960 minutes of annealing

while the 1. order fits better for the values measured 24 hours after annealing, a period during which they were stored at room temperature. Fig. 15 shows ΔN_{eff} for the device CA0510 with the assumption that the device is inverted from the beginning. In contrast to that Fig. 16 shows ΔN_{eff} for the same device if it is assumed that the device is inverted after 60 minutes of annealing. For this plot it was necessary to leave out from the fit some measured points close to the inversion time. The values obtained for the fit parameters are listed in Tab. 5, if it is assumed that the devices are inverted from the beginning, and for the assumption of later inversion in Tab. 6

Device \ Parameter	N_c	N_a	N_y	τ_1 [min]	τ_2 [min]
CA0510 1. order	1,068	0,295	0,542	27,764	200,75
CA0510 2. order	0,2499	1,102	1,408	28,667	40,123
CD1710 1. order	0,763	0,293	0,156	33,41	100,79
CD1710 2. order	0,807	0,251	0,127	28,113	99,89

Table 5: Values of parameters for ΔN_{eff} if devices are inverted from beginning; the units of N_c, N_a, N_y are 10^{11}cm^{-3}

Device \ Parameter	N_c	N_a	N_y	τ_1 [min]	τ_2 [min]
CA0510 1. order	0,912	0,0	0,686	97,40	138,3
CA0510 2. order	0,898	0,0	0,781	17,79	105,02
CD1710 1. order	0,522	0,0	0,399	1,0	76,81
CD1710 2. order	0,511	0,0	0,444	1,0	56,91

Table 6: Values of parameters for ΔN_{eff} if devices are inverted from beginning; the units of N_c, N_a, N_y are 10^{11}cm^{-3}

Fig. 17 and Fig. 18 show the same plots for the device CD1710. Here it is assumed that the device is inverted after 90 minutes of annealing. Here it was also necessary to leave out some points close to the inversion time.

In Fig. 19 the relation between N_{eff} and the fluence is plotted, assuming that the devices irradiated at the higher fluence are inverted after irradiation also before annealing. The values of N_{eff} are therefore negative at the higher fluence. The experimental points have been fitted using the following equation:

$$N_{eff} = N_{eff,0} \cdot \exp\left(-c \cdot \Phi_{el}\right) - g_c \cdot \Phi_{el}$$

The values of the parameters calculated from the fit are displayed in Tab. 7.

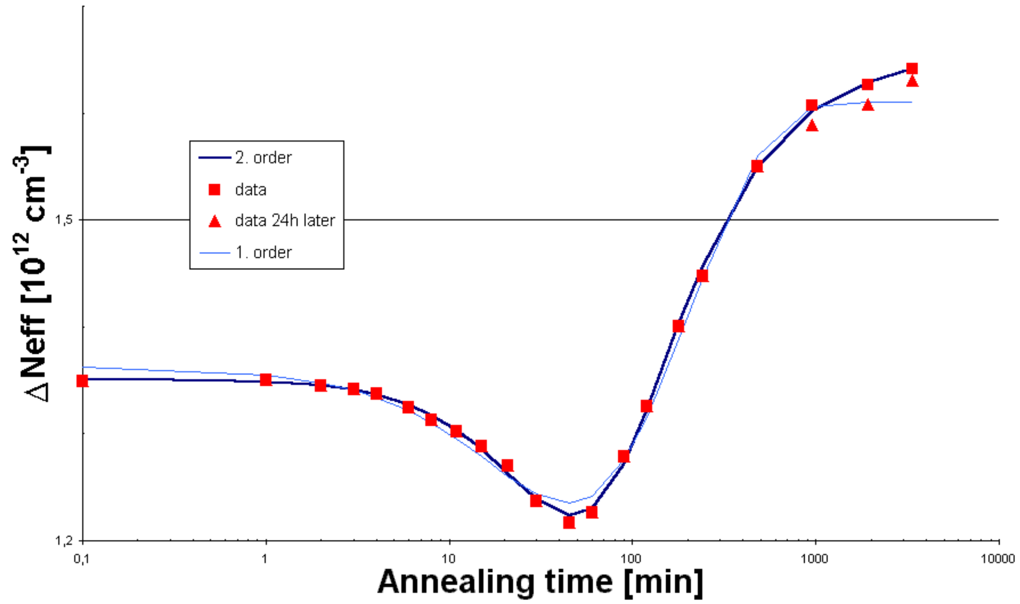

Figure 15: ΔN_{eff} of CA0510, if inverted from the beginning

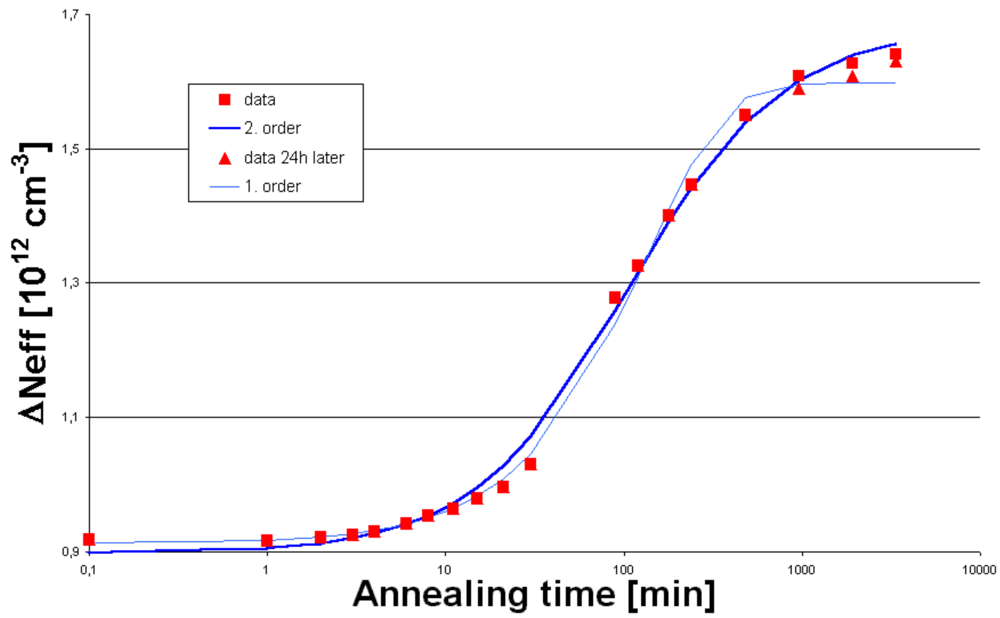

Figure 16: ΔN_{eff} of CA0510, if inverted after 60 minutes of annealing

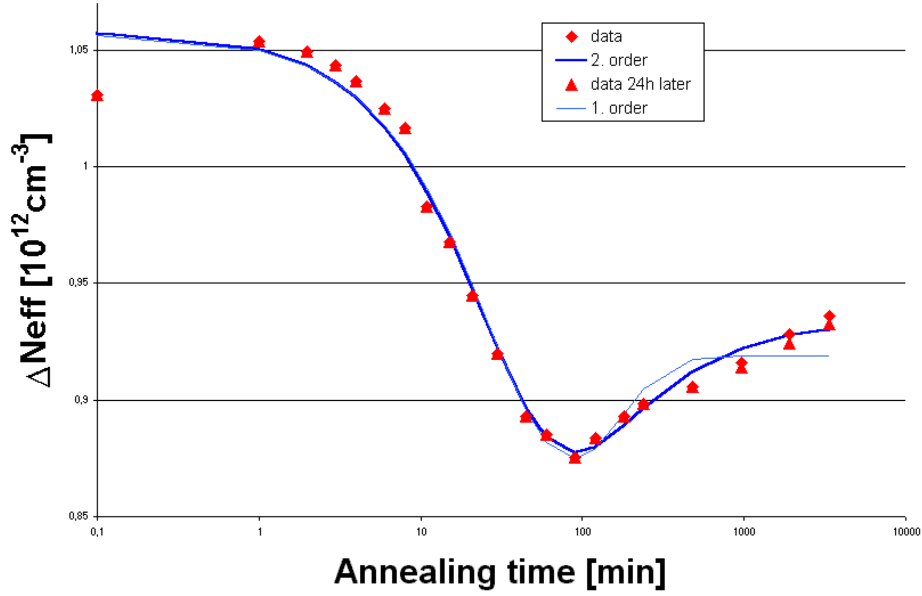

Figure 17: ΔN_{eff} of CD1710, if inverted from the beginning

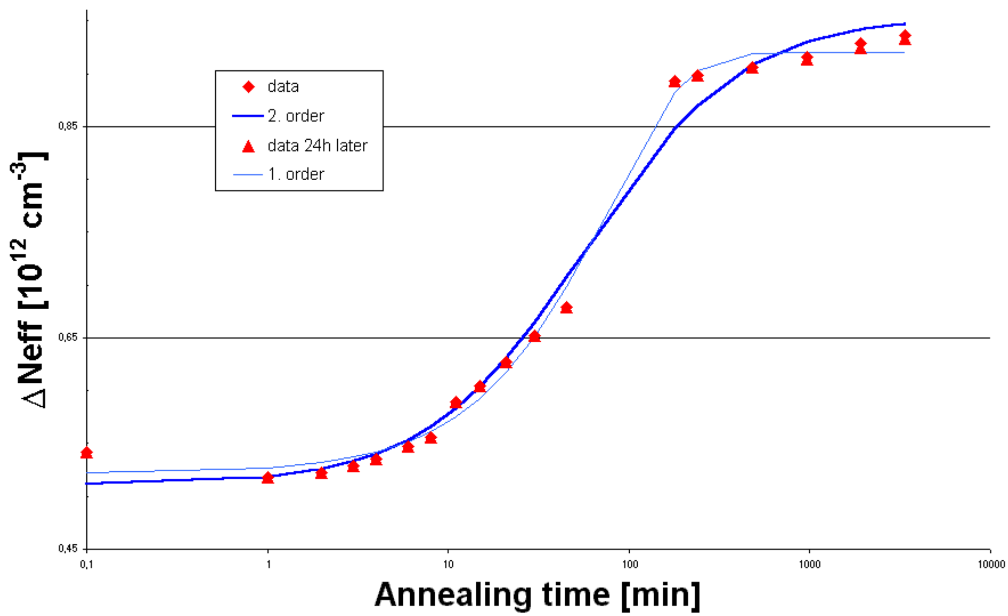

Figure 18: ΔN_{eff} of CD1710, if inverted after 90 minutes of annealing

Device \ Parameter	c $[10^{-3}\text{cm}^{-1}]$	g_c $[10^{-14}\text{cm}^2]$
CA	0,3619	0,0
CD	0,2601	0,0

Table 7: Values of parameters for the fit of ΔN_{eff} as a function of the fluence

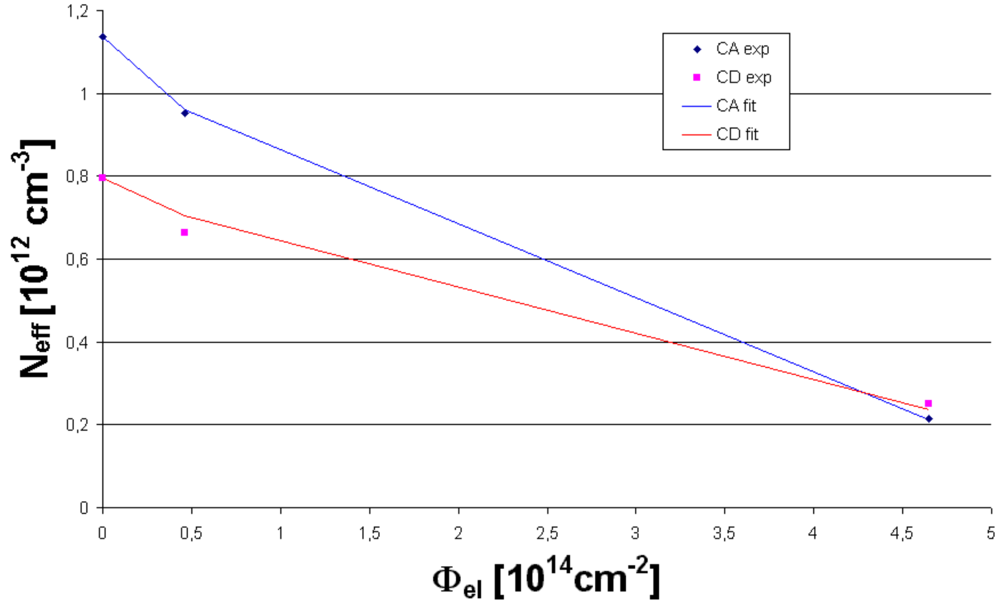

Figure 19: N_{eff} relation to the fluence

Unfortunately the devices have been irradiated only with two different fluences, so that the curve has only three points to fix. For this reason it is not possible to take many information out of this plot.

5 Conclusions

In this work we studied the radiation tolerance of two different silicon materials (Float Zone (FZ) and Diffusion Oxygenated Float Zone (DOFZ)) after low energy (15MeV) electron irradiation up to a fluence of 4,65 electrons/cm^2. Irradiated devices have been annealed at 80 ℃ up to 3360 minutes (equal to 187 days at room temperature) and standard CV/IV measurements have been performed at different annealing times. Transient Current Technique (TCT) measurements have also been performed in order to determine the sign of the electric field and therefore the eventual type inversion in irradiated devices.

For all devices it was observed that the depletion voltage decreases after irradiation, even if it was not possible to state if substrate type inversion occurred or not soon after irradiation. Devices irradiated at the higher fluence anyway showed type inversion after annealing at 80 ℃ , respectively at around 60 minutes for FZ and later (90 minutes) for DOFZ.
The evolution of ΔN_{eff} for these devices as a function of the annealing time was parameterised by means of a theoretical model (the "Hamburg model"). As for the devices irradiated at the lower fluence, only a slight decrease of the depletion voltage was observed as a function of the annealing time.
Finally the hardness factor κ of 15 MeV electrons has been calculated from the experimental data and found to be equal to $\sim 0,02$.

References

- H. Feick: *Radiation Tolerance of Silicon Particle Detectors for High-Energy Physics Expermiments*, PHD thesis Hamburg 1997
- M. Moll *Radiation Damage in Silicon Particle Detectors*, PHD thesis Hamburg 1999
- G. Kramberger: *Signal development in irradiated silicon detectors*, PHD thesis Ljubljana 2001
- G. Lindström: *Radiation damage in silicon detectors*, to be published in NIMA 2003